

Spatial two-photon coherence of the entangled field produced by down-conversion using a partially spatially coherent pump beam

Anand Kumar Jha* and Robert W. Boyd†

The Institute of Optics, University of Rochester, Rochester, New York 14627, USA

(Received 14 September 2009; published 27 January 2010)

We study the spatial coherence properties of the entangled two-photon field produced by parametric down-conversion (PDC) when the pump field is, spatially, a partially coherent beam. By explicitly treating the case of a pump beam of the Gaussian Schell-model type, we show that in PDC the spatial coherence properties of the pump field get entirely transferred to the spatial coherence properties of the down-converted two-photon field. As one important consequence of this study, we find that, for two-qubit states based on the position correlations of the two-photon field, the maximum achievable entanglement, as quantified by concurrence, is bounded by the degree of spatial coherence of the pump field. These results could be important by providing a means of controlling the entanglement of down-converted photons by tailoring the degree of coherence of the pump field.

DOI: [10.1103/PhysRevA.81.013828](https://doi.org/10.1103/PhysRevA.81.013828)

PACS number(s): 42.50.Ar, 03.67.Mn, 42.65.Lm, 03.65.Ud

I. INTRODUCTION

In the past few decades several temporal [1–9] and spatial [10–17] interference effects have been observed with the entangled two-photon field produced by parametric down-conversion (PDC)—a nonlinear optical process in which a pump photon interacts with a crystal and splits into two separate photons called the signal and idler photons. The coherence properties of the two-photon field are affected by the crystal parameters as well as by the pump field parameters and have been studied in various different contexts [18–24]. In particular, it has been shown that the angular spectrum of the pump field gets completely transferred to the down-converted two-photon field [20]. In all these previous studies [10–24], the pump field has been taken to be spatially coherent, and the effects due to the limited spatial coherence of the pump field have so far not been investigated. In this article, we study how the spatial coherence properties of the pump field affect the spatial coherence properties of the entangled two-photon field.

The article is organized as follows. In Sec. II, we present a conceptual description of spatial two-photon interference in terms of two displacement parameters, which we construct using the transverse position vectors of the signal and idler photons in the two interfering alternatives. In Sec. III, taking the pump field to be a partially coherent Gaussian Schell-model beam [25–27], we show in terms of the two displacement parameters that the spatial coherence properties of the pump field get entirely transferred to the down-converted two-photon field. In Sec. IV, we discuss the effects due to the limited spatial coherence of the pump field on the entanglement of two-qubit states that are based on the position correlations of the down-converted photons. We show that the maximum achievable entanglement of such states, as quantified by concurrence, is bounded by the degree of spatial coherence of the pump field. Sec. V presents some conclusions.

II. SPATIAL TWO-PHOTON INTERFERENCE: CONCEPTUAL DESCRIPTION

Figure 1 represents a generic situation for studying the spatial coherence properties of the two-photon field. The signal and idler photons produced by PDC go through a pair of double holes located at plane z . They are detected in coincidence by detectors D_s and D_i located at positions \mathbf{r}_s and \mathbf{r}_i , respectively. There are two alternative pathways by which signal and idler photons can reach detectors D_s and D_i . In alternative 1, the signal and idler photons go through the pair of holes located at $\mathbf{r}_{s1} \equiv (\boldsymbol{\rho}_{s1}, z)$ and $\mathbf{r}_{i1} \equiv (\boldsymbol{\rho}_{i1}, z)$, and in alternative 2, they go through those located at $\mathbf{r}_{s2} \equiv (\boldsymbol{\rho}_{s2}, z)$ and $\mathbf{r}_{i2} \equiv (\boldsymbol{\rho}_{i2}, z)$. In principle, there are two more alternative pathways: one in which the signal and idler photons go through the pair of holes located at $\mathbf{r}_{s1} \equiv (\boldsymbol{\rho}_{s1}, z)$ and $\mathbf{r}_{i2} \equiv (\boldsymbol{\rho}_{i2}, z)$, and the second in which they go through those located at $\mathbf{r}_{s2} \equiv (\boldsymbol{\rho}_{s2}, z)$ and $\mathbf{r}_{i1} \equiv (\boldsymbol{\rho}_{i1}, z)$. In what follows we explicitly assume that the phase-matching condition is such that the probability amplitudes of these two other alternatives are negligibly small.

Throughout this article, subscripts p , s , and i stand for pump, signal, and idler, respectively. In Fig. 1, the distance traveled by a photon from the crystal to a hole is denoted by r . The distance traveled from a hole to the corresponding detector is denoted by d and the associated time elapsed by $t = d/c$. The transverse position vector of a photon is denoted by $\boldsymbol{\rho}$. Thus, $\boldsymbol{\rho}_{s1}$ represents the transverse position vector of the signal photon in alternative 1, etc. We define two displacement parameters in terms of the transverse position vectors of the signal and idler photons in the two alternatives as

$$\begin{aligned} \boldsymbol{\rho}_1 &\equiv \frac{\boldsymbol{\rho}_{s1} + \boldsymbol{\rho}_{i1}}{2}, & \boldsymbol{\rho}_2 &\equiv \frac{\boldsymbol{\rho}_{s2} + \boldsymbol{\rho}_{i2}}{2}, & \Delta\boldsymbol{\rho} &= \boldsymbol{\rho}_1 - \boldsymbol{\rho}_2 \\ \boldsymbol{\rho}'_1 &\equiv \boldsymbol{\rho}_{s1} - \boldsymbol{\rho}_{i1}, & \boldsymbol{\rho}'_2 &\equiv \boldsymbol{\rho}_{s2} - \boldsymbol{\rho}_{i2}, & \Delta\boldsymbol{\rho}' &= \boldsymbol{\rho}'_1 - \boldsymbol{\rho}'_2. \end{aligned} \quad (1)$$

Here $\boldsymbol{\rho}_{1(2)}$ and $\boldsymbol{\rho}'_{1(2)}$ are the two-photon transverse position vector and the two-photon position-asymmetry vector in alternative 1 (2). For either alternative, the two-photon transverse position vector is defined to be the average of the transverse position vectors of the signal and idler photons; the two-photon position-asymmetry vector is defined to be the difference of the transverse position vectors of the signal and idler photons.

*anand@optics.rochester.edu

†boydrw@mac.com

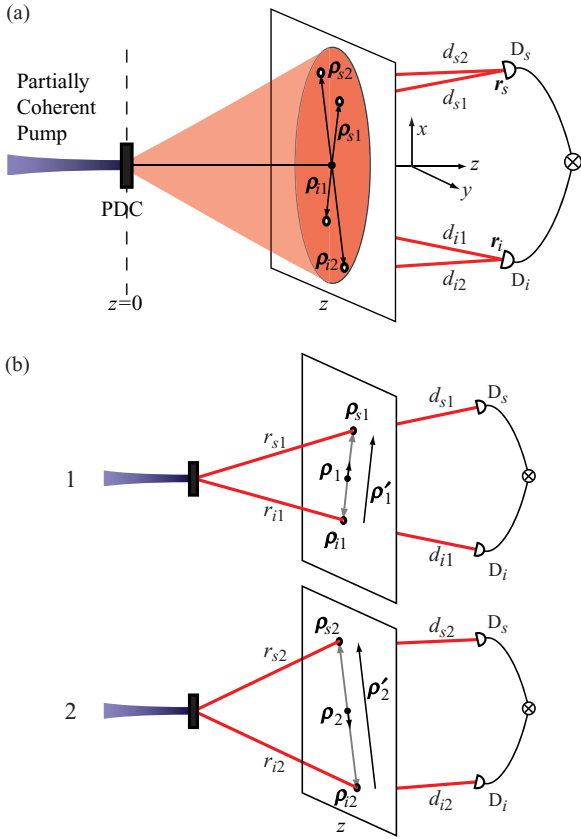


FIG. 1. (Color online) (a) Schematic laboratory setup that could be used to study the spatial coherence properties of the two-photon field produced by PDC using a partially coherent pump beam. (b) 1 and 2 represent two alternative pathways by which the down-converted signal and idler photons can pass through the holes and get detected in coincidence at detectors D_s and D_i . In alternative 1, the signal and idler photons go through the pair of holes located at $\mathbf{r}_{s1} \equiv (\boldsymbol{\rho}_{s1}, z)$ and $\mathbf{r}_{i1} \equiv (\boldsymbol{\rho}_{i1}, z)$, and in alternative 2, they go through those located at $\mathbf{r}_{s2} \equiv (\boldsymbol{\rho}_{s2}, z)$ and $\mathbf{r}_{i2} \equiv (\boldsymbol{\rho}_{i2}, z)$. $\boldsymbol{\rho}_{1(2)}$ and $\boldsymbol{\rho}'_{1(2)}$ are the two displacement parameters in alternatives 1 (2) defined in Eq. (1) in terms of which we describe the coherence properties of the two-photon field.

We denote the positive-frequency parts of the electric fields at detectors D_s and D_i by $\hat{E}_s^{(+)}(\mathbf{r}_s, t)$ and $\hat{E}_i^{(+)}(\mathbf{r}_i, t)$, respectively. $\hat{E}_s^{(+)}(\mathbf{r}_s, t)$ and $\hat{E}_i^{(+)}(\mathbf{r}_i, t)$ are equal to the sum of the signal and idler fields arriving at detectors D_s and D_i in alternatives 1 and 2; that is,

$$\hat{E}_s^{(+)}(\mathbf{r}_s, t) = k_{s1} \hat{E}_{s1}^{(+)}(\mathbf{r}_{s1}) e^{-i\omega_s(t-t_{s1})} + k_{s2} \hat{E}_{s2}^{(+)}(\mathbf{r}_{s2}) e^{-i\omega_s(t-t_{s2})}, \quad (2)$$

$$\hat{E}_i^{(+)}(\mathbf{r}_i, t) = k_{i1} \hat{E}_{i1}^{(+)}(\mathbf{r}_{i1}) e^{-i\omega_i(t-t_{i1})} + k_{i2} \hat{E}_{i2}^{(+)}(\mathbf{r}_{i2}) e^{-i\omega_i(t-t_{i2})}. \quad (3)$$

Here $\hat{E}_{s1}^{(+)}(\mathbf{r}_{s1})$ is the positive-frequency part of the signal field at position \mathbf{r}_{s1} , etc. The constant factor k_{s1} depends on the size of the hole at \mathbf{r}_{s1} and the geometry of the arrangement. The coincidence count rate $R_{si}(\mathbf{r}_s, \mathbf{r}_i)$, which is the probability per (unit time)² that a photon is detected at position \mathbf{r}_s at time t and another at position \mathbf{r}_i at time $t + \tau$, is given by $R_{si}(\mathbf{r}_s, \mathbf{r}_i) = \alpha_s \alpha_i \text{tr}\{\rho_{\text{tp}} \hat{E}_s^{(-)}(\mathbf{r}_s, t) \hat{E}_i^{(-)}(\mathbf{r}_i, t + \tau)\}$, where the symbol tr stands for the trace, α_s and α_i denote the quantum efficiencies of detectors D_s and D_i , respectively, and ρ_{tp} represents the density matrix of the two-photon field produced by PDC. By substituting from Eqs. (2) and (3), we write the coincidence count rate $R_{si}(\mathbf{r}_s, \mathbf{r}_i)$ as

$R_{si}(\mathbf{r}_s, \mathbf{r}_i) = k_1^2 S^{(2)}(\boldsymbol{\rho}_{s1}, \boldsymbol{\rho}_{i1}, z) + k_2^2 S^{(2)}(\boldsymbol{\rho}_{s2}, \boldsymbol{\rho}_{i2}, z) + k_1 k_2 W^{(2)}(\boldsymbol{\rho}_{s1}, \boldsymbol{\rho}_{i1}, \boldsymbol{\rho}_{s2}, \boldsymbol{\rho}_{i2}, z) \times e^{i[\omega_s(t_{s1}-t_{s2}) + \omega_i(t_{i1}-t_{i2})]} + \text{c.c.}, \quad (4a)$

$$R_{si}(\mathbf{r}_s, \mathbf{r}_i) = k_1^2 S^{(2)}(\boldsymbol{\rho}_{s1}, \boldsymbol{\rho}_{i1}, z) + k_2^2 S^{(2)}(\boldsymbol{\rho}_{s2}, \boldsymbol{\rho}_{i2}, z) + k_1 k_2 W^{(2)}(\boldsymbol{\rho}_{s1}, \boldsymbol{\rho}_{i1}, \boldsymbol{\rho}_{s2}, \boldsymbol{\rho}_{i2}, z) \times e^{i[\omega_s(t_{s1}-t_{s2}) + \omega_i(t_{i1}-t_{i2})]} + \text{c.c.}, \quad (4a)$$

where $k_1 = \sqrt{\alpha_s \alpha_i} k_{s1} k_{i1}$, $k_2 = \sqrt{\alpha_s \alpha_i} k_{s2} k_{i2}$,

$$W^{(2)}(\boldsymbol{\rho}_{s1}, \boldsymbol{\rho}_{i1}, \boldsymbol{\rho}_{s2}, \boldsymbol{\rho}_{i2}, z) = \text{tr}\{\rho_{\text{tp}} \hat{E}_{s1}^{(-)}(\mathbf{r}_{s1}) \hat{E}_{i1}^{(-)}(\mathbf{r}_{i1}) \hat{E}_{i2}^{(+)}(\mathbf{r}_{i2}) \hat{E}_{s2}^{(+)}(\mathbf{r}_{s2})\} \quad (4b)$$

and

$$S^{(2)}(\boldsymbol{\rho}_{s1}, \boldsymbol{\rho}_{i1}, z) = W^{(2)}(\boldsymbol{\rho}_{s1}, \boldsymbol{\rho}_{i1}, \boldsymbol{\rho}_{s1}, \boldsymbol{\rho}_{i1}, z). \quad (4c)$$

Equation (4a) is the interference law for the two-photon field. The first and second terms of Eq. (4a) are the coincidence count rates when coincidences are collected from only alternatives 1 and 2, respectively. The interference terms appear when coincidences are collected from both the alternatives. $S^{(2)}(\boldsymbol{\rho}_{s1}, \boldsymbol{\rho}_{i1}, z)$ and $S^{(2)}(\boldsymbol{\rho}_{s2}, \boldsymbol{\rho}_{i2}, z)$ will be referred to as the two-photon spectral density in alternatives 1 and 2, respectively; these terms are recognized as the two-photon analogs of the spectral density function of the second-order coherence theory [27]. $W^{(2)}(\boldsymbol{\rho}_{s1}, \boldsymbol{\rho}_{i1}, \boldsymbol{\rho}_{s2}, \boldsymbol{\rho}_{i2}, z)$ will be referred to as the two-photon cross-spectral density function; it is a four-point fourth-order (in the field) correlation function. It satisfies four Wolf equations [24,27,28] and is recognized as the two-photon analog of the cross-spectral density function. To keep the notations simpler, we do not show the frequency arguments in the definitions of the two-photon spectral density and the two-photon cross-spectral density functions.

III. THE SPATIAL COHERENCE PROPERTIES OF THE TWO-PHOTON FIELD

We evaluate the two-photon cross-spectral density function $W^{(2)}(\boldsymbol{\rho}_{s1}, \boldsymbol{\rho}_{i1}, \boldsymbol{\rho}_{s2}, \boldsymbol{\rho}_{i2}, z)$, and thereby the coincidence count rate $R_{si}(\mathbf{r}_s, \mathbf{r}_i)$, in terms of the two displacement parameters defined in Eq. (1). For conceptual clarity, and without any loss of generality, we assume that the pump, signal, and idler fields are monochromatic, with frequencies given by ω_0 , ω_s , and ω_i , respectively. We take the down-conversion crystal to be very thin and assume paraxial conditions. The state of the two-photon field produced by PDC can then be represented by a density matrix ρ_{tp} given by [18–20]:

$$\rho_{\text{tp}} = |A|^2 \iiint \int d\mathbf{q}_s d\mathbf{q}_i d\mathbf{q}'_s d\mathbf{q}'_i \times \langle V(\mathbf{q}_s + \mathbf{q}_i) V^*(\mathbf{q}'_s + \mathbf{q}'_i) \rangle_e |\mathbf{q}_s\rangle |\mathbf{q}_i\rangle \langle \mathbf{q}'_s| \langle \mathbf{q}'_i|, \quad (5)$$

where $|A|^2$ is a constant that depends on physical constants, $\langle \dots \rangle_e$ represents the ensemble average over the different realizations of the pump field, and \mathbf{q}_s and \mathbf{q}_i are the transverse wave vectors of the signal and idler fields. The ensemble average $\langle V(\mathbf{q}_s + \mathbf{q}_i) V^*(\mathbf{q}'_s + \mathbf{q}'_i) \rangle_e$ is recognized as the angular correlation function of the pump field [29], with $\mathbf{q}_s + \mathbf{q}_i = \mathbf{q}_p$

and $\mathbf{q}'_s + \mathbf{q}'_i = \mathbf{q}'_p$ being the transverse wave vectors of the pump field. In writing Eq. (5), it has been assumed that the pump field intensities are so weak that effects that occur at high pump intensities, such as the gain-induced diffraction [30], have no appreciable effect on the generated two-photon field.

The electric field operators $\hat{E}^{(+)}(\mathbf{r}_{s1})$ and $\hat{E}^{(+)}(\mathbf{r}_{i1})$, within the paraxial approximations, can be written as [18–20]

$$\hat{E}_{s1}^{(+)}(\mathbf{r}_{s1}) = e^{ik_s z} \int d\mathbf{q} \hat{a}_s(\mathbf{q}) e^{i(\mathbf{q} \cdot \boldsymbol{\rho}_{s1} - q^2 z / 2k_s)}, \quad (6)$$

$$\hat{E}_{i1}^{(+)}(\mathbf{r}_{i1}) = e^{ik_i z} \int d\mathbf{q}' \hat{a}_i(\mathbf{q}') e^{i(\mathbf{q}' \cdot \boldsymbol{\rho}_{i1} - q'^2 z / 2k_i)}, \quad (7)$$

where $q^2 = |\mathbf{q}|^2$, $q'^2 = |\mathbf{q}'|^2$, $k_s = \mathbf{k}_s(\omega_s)$, and $k_i = \mathbf{k}_i(\omega_i)$. We present in this section our calculations for the case of degenerate down-conversion only; the nondegenerate case is presented in the Appendix. We take $\omega_s = \omega_i = \omega_0/2$ and, within the paraxial approximations, take $k_s \approx k_i \approx k_0/2$, where k_0 is the central wave-vector magnitude of the pump field. Using Eqs. (5), (6), and (7), we write Eq. (4b) as

$$\begin{aligned} & W^{(2)}(\boldsymbol{\rho}_{s1}, \boldsymbol{\rho}_{i1}, \boldsymbol{\rho}_{s2}, \boldsymbol{\rho}_{i2}, z) \\ &= |A|^2 \iiint d\mathbf{q}_s d\mathbf{q}'_s d\mathbf{q}_i d\mathbf{q}'_i \\ & \times \langle V(\mathbf{q}_s + \mathbf{q}_i) V^*(\mathbf{q}'_s + \mathbf{q}'_i) \rangle e^{i[\mathbf{q}_s \cdot \boldsymbol{\rho}_{s1} + \mathbf{q}_i \cdot \boldsymbol{\rho}_{i1} - \mathbf{q}'_s \cdot \boldsymbol{\rho}_{s2} - \mathbf{q}'_i \cdot \boldsymbol{\rho}_{i2}]} \\ & \times e^{-i(z/k_0)[(q_s^2 + q_i^2) - (q_s'^2 + q_i'^2)]}. \end{aligned} \quad (8)$$

The two-photon cross-spectral density function $W^{(2)}(\boldsymbol{\rho}_{s1}, \boldsymbol{\rho}_{i1}, \boldsymbol{\rho}_{s2}, \boldsymbol{\rho}_{i2}, z)$ is an integral of the angular correlation function of the pump field; and therefore, the spatial coherence properties of the pump field get transferred to the spatial coherence properties of the two-photon field. We calculate the analytical expression for the two-photon cross-spectral density, for the special case of a partially coherent pump field of Gaussian Schell-model type [25].

A Gaussian Schell-model beam is characterized by its beam waist width σ_s at $z = 0$ and its transverse coherence width σ_μ at $z = 0$, which is the distance scale over which the pump field at $z = 0$ remains spatially coherent. The angular correlation function for the Gaussian Schell-model pump field is given by (see Ref. [26], Section 5.6.4)

$$\begin{aligned} & \langle V(\mathbf{q}_s + \mathbf{q}_i) V^*(\mathbf{q}'_s + \mathbf{q}'_i) \rangle_e \\ & \rightarrow \langle V(\mathbf{q}_p) V^*(\mathbf{q}'_p) \rangle_e \\ &= (A_p \sigma_s \delta / 2\pi)^2 \exp[-\alpha(q_p)^2 - \alpha(q'_p)^2 + 2\beta \mathbf{q}_p \cdot \mathbf{q}'_p], \end{aligned} \quad (9a)$$

where

$$\begin{aligned} \alpha &= \sigma_s^2 (\sigma_\mu^2 + 2\sigma_s^2) / (\sigma_\mu^2 + 4\sigma_s^2), \\ \beta &= 2\sigma_s^4 / (\sigma_\mu^2 + 4\sigma_s^2), \\ \delta^2 &= 4\sigma_s^2 \sigma_\mu^2 / (\sigma_\mu^2 + 4\sigma_s^2), \end{aligned} \quad (9b)$$

and A_p is a constant. The far-field expression of the cross-spectral density function $W(\boldsymbol{\rho}_{p1}, \boldsymbol{\rho}_{p2}, z)$ of the pump field at positions $\mathbf{r}_{p1} \equiv (\boldsymbol{\rho}_{p1}, z)$ and $\mathbf{r}_{p2} \equiv (\boldsymbol{\rho}_{p2}, z)$ along the pump beam path is then given by (see Ref. [26], section 5.6.4)

$$\begin{aligned} W(\boldsymbol{\rho}_{p1}, \boldsymbol{\rho}_{p2}, z) &= e^{ik_0(r_{p1} - r_{p2})} \\ & \times \sqrt{S(\boldsymbol{\rho}_{p1}, z) S(\boldsymbol{\rho}_{p2}, z)} \mu(\Delta\boldsymbol{\rho}_p, z), \end{aligned} \quad (10a)$$

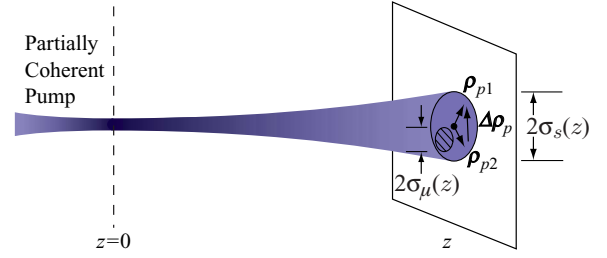


FIG. 2. (Color online) Schematic representation of a partially spatially coherent pump beam; $\sigma_s(z)$ is the rms beam radius of the pump field at plane z and $\sigma_\mu(z)$ is the rms spatial coherence width of the pump field at plane z . $\boldsymbol{\rho}_{p1}$ and $\boldsymbol{\rho}_{p2}$ are the transverse position vectors of two points within the pump beam.

where $r_{p1} = |\mathbf{r}_{p1}|$, $r_{p2} = |\mathbf{r}_{p2}|$ and $\Delta\boldsymbol{\rho}_p = \boldsymbol{\rho}_{p1} - \boldsymbol{\rho}_{p2}$;

$$S(\boldsymbol{\rho}_{p1}, z) = (A_p \sigma_s \delta k_0 / z)^2 \exp\{-(1/2)[\rho_{p1} / \sigma_s(z)]^2\} \quad (10b)$$

is the spectral density of the pump field at position \mathbf{r}_{p1} , with

$$\sigma_s(z) = z \sqrt{\sigma_\mu^2 + 4\sigma_s^2} / 2k_0 \sigma_s \sigma_\mu \quad (10c)$$

being the rms beam radius of the pump field at plane z in the far field; and

$$\mu(\Delta\boldsymbol{\rho}_p, z) = \exp\{-(1/2)[\Delta\rho_p / \sigma_\mu(z)]^2\} \quad (10d)$$

is the degree of spatial coherence of the pump field, with

$$\sigma_\mu(z) = z \sqrt{\sigma_\mu^2 + 4\sigma_s^2} / 2k_0 \sigma_s^2 \quad (10e)$$

being the rms spatial coherence width of the pump field at plane z in the far field. Figure 2 illustrates the beam radius $\sigma_s(z)$ and the spatial coherence width $\sigma_\mu(z)$ of a partially coherent pump beam.

We now substitute Eq. (9) into Eq. (8) and calculate the far-field expression of the two-photon cross-spectral density $W^{(2)}(\boldsymbol{\rho}_{s1}, \boldsymbol{\rho}_{i1}, \boldsymbol{\rho}_{s2}, \boldsymbol{\rho}_{i2}, z)$. After a very long but straightforward calculation, we find that

$$\begin{aligned} & W^{(2)}(\boldsymbol{\rho}_{s1}, \boldsymbol{\rho}_{i1}, \boldsymbol{\rho}_{s2}, \boldsymbol{\rho}_{i2}, z) \\ &= C \exp[(ik_0/4z)(\rho_{s1}^2 + \rho_{i1}^2 - \rho_{s2}^2 - \rho_{i2}^2)] \\ & \times \exp\{-(\alpha k_0^2/4z^2)[(\rho_{s1} + \rho_{i1})^2 + (\rho_{s2} + \rho_{i2})^2] \\ & + (\beta k_0^2/2z^2)[(\rho_{s1} + \rho_{i1}) \cdot (\rho_{s2} + \rho_{i2})]\}, \end{aligned} \quad (11)$$

where $C = |A|^2 [(A_p \pi \sigma_s \delta k_0^2) / (2z^2)]^2$ and $\rho_{s1} = |\boldsymbol{\rho}_{s1}|$ is the distance from the z axis of the hole located at \mathbf{r}_{s1} , etc. Since the distances of the holes from the z axis were assumed to be much smaller than their distances from the crystal, we make the approximation $r_{s1} \approx z + \rho_{s1}^2 / 2z$, etc., and write $(1/2z)(\rho_{s1}^2 + \rho_{i1}^2 - \rho_{s2}^2 - \rho_{i2}^2) \approx (r_{s1} + r_{i1} - r_{s2} - r_{i2})$. Next, we substitute $r_1 = (r_{s1} + r_{i1})/2$ and $r_2 = (r_{s2} + r_{i2})/2$ and write down $W^{(2)}(\boldsymbol{\rho}_{s1}, \boldsymbol{\rho}_{i1}, \boldsymbol{\rho}_{s2}, \boldsymbol{\rho}_{i2}, z)$ in terms of the two-photon transverse position vectors defined in Eq. (1). We then obtain

$$\begin{aligned} & W^{(2)}(\boldsymbol{\rho}_{s1}, \boldsymbol{\rho}_{i1}, \boldsymbol{\rho}_{s2}, \boldsymbol{\rho}_{i2}, z) \\ & \rightarrow W^{(2)}(\boldsymbol{\rho}_1, \boldsymbol{\rho}_2, z) \\ &= e^{ik_0(r_1 - r_2)} \sqrt{S^{(2)}(\boldsymbol{\rho}_1, z) S^{(2)}(\boldsymbol{\rho}_2, z)} \mu^{(2)}(\Delta\boldsymbol{\rho}, z), \end{aligned} \quad (12a)$$

where

$$S^{(2)}(\boldsymbol{\rho}_1, z) = C \exp\{-(1/2)[\rho_1 / \sigma_s^{(2)}(z)]^2\} \quad (12b)$$

is the two-photon spectral density in alternative 1, with

$$\sigma_s^{(2)}(z) = z\sqrt{\sigma_\mu^2 + 4\sigma_s^2}/2k_0\sigma_s\sigma_\mu \quad (12c)$$

being the rms correlation width of the two-photon field at z ; and where

$$\mu^{(2)}(\Delta\rho, z) = \exp\left\{-(1/2)[\Delta\rho/\sigma_\mu^{(2)}(z)]^2\right\} \quad (12d)$$

is the degree of spatial two-photon-coherence, with

$$\sigma_\mu^{(2)}(z) = z\sqrt{\sigma_\mu^2 + 4\sigma_s^2}/2k_0\sigma_s^2 \quad (12e)$$

being the rms spatial coherence width of the two-photon field. Comparing Eqs. (10) and (12), we at once find that in terms of the two-photon transverse position vectors, the two-photon cross-spectral density function assumes the same form as does the pump cross-spectral density function in terms of the pump transverse position vectors. Thus, the spatial coherence properties of the pump field get entirely transferred to the spatial coherence properties of the down-converted two-photon field. We note that the functional forms of the two-photon correlation width $\sigma_s^{(2)}(z)$ and the two-photon transverse coherence width $\sigma_\mu^{(2)}(z)$ are the same as those of the pump beam radius $\sigma_s(z)$ and the pump transverse coherence width $\sigma_\mu(z)$, respectively. Thus, the two-photon field seems to propagate as if it were the pump beam with its transverse position vectors given by the two-photon transverse position vectors. Figure 3 illustrates the physical interpretation of the two-photon correlation width and the two-photon transverse coherence width.

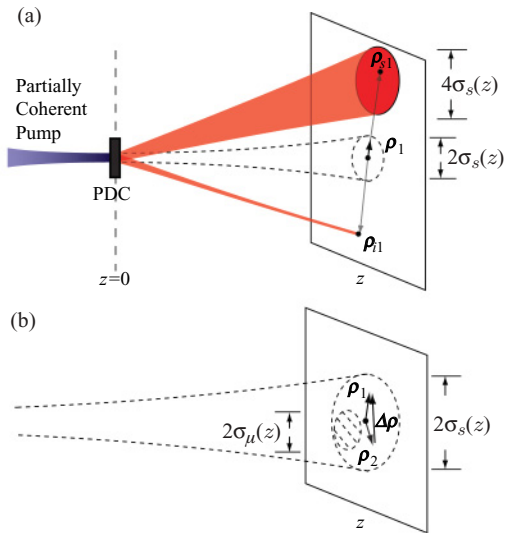


FIG. 3. (Color online) Physical interpretation of the two-photon correlation width $\sigma_s^{(2)}(z)$ and the two-photon transverse coherence width $\sigma_\mu^{(2)}(z)$ in terms of the two-photon transverse position vectors. (a) The two-photon correlation width $\sigma_s^{(2)}(z)$ is equal to the pump beam radius $\sigma_s(z)$. As a result, when an idler photon is detected at position ρ_{i1} , the corresponding signal photon has an appreciable probability of being detected anywhere inside an area whose center is at $-\rho_{i1}$ and whose radius is twice the pump beam radius $\sigma_s(z)$. (b) The two-photon spatial coherence width $\sigma_\mu^{(2)}(z)$ is equal to the spatial coherence width of the pump field $\sigma_\mu(z)$; thus, for alternatives 1 and 2 of Fig. 1 to remain mutually coherent, $|\Delta\rho| = |\rho_1 - \rho_2|$ has to be less than the spatial coherence width $\sigma_\mu(z)$ of the pump field.

The coincidence count rate $R_{si}(\mathbf{r}_s, \mathbf{r}_i)$ of Eq. (4a) can now be written as

$$\begin{aligned} R_{si}(\mathbf{r}_s, \mathbf{r}_i) &= k_1^2 S^{(2)}(\rho_1, z) + k_2^2 S^{(2)}(\rho_2, z) \\ &\quad + 2k_1 k_2 \sqrt{S^{(2)}(\rho_1, z) S^{(2)}(\rho_2, z)} \mu^{(2)}(\Delta\rho, z) \cos(k_0 \Delta L), \end{aligned} \quad (13)$$

where we have replaced $\omega_0 t_{s1}$ by $k_0 d_{s1}$, etc., and have substituted $l_1 = r_1 + (d_{s1} + d_{i1})/2$, $l_2 = r_2 + (d_{s2} + d_{i2})/2$ and $\Delta L = l_1 - l_2$. Here $l_{1(2)}$ is the two-photon path-length in alternative 1 (2) [7,31]. The visibility V of the two-photon interference fringes is given by

$$V = \frac{2k_1 k_2 \sqrt{S^{(2)}(\rho_1, z) S^{(2)}(\rho_2, z)}}{k_1^2 S^{(2)}(\rho_1, z) + k_2^2 S^{(2)}(\rho_2, z)} \mu^{(2)}(\Delta\rho, z). \quad (14)$$

We note that the two-photon cross-spectral density function [Eq. (12a)] and the coincidence count rate [Eq. (13)] depend on only one displacement parameter, the two-photon transverse position vector, and remain independent of the other displacement parameter, the two-photon position-asymmetry vector. This is a special feature of the degenerate two-photon field. However, in the case of nondegenerate two-photon fields, the two-photon cross-spectral density depends on both the displacement parameters, as we show in the Appendix.

IV. SPATIAL TWO-PHOTON COHERENCE AND ENTANGLEMENT OF SPATIAL TWO-QUBIT STATES

Two-qubit states are very important for quantum information technology, as they are the necessary ingredients for many quantum information based applications, such as quantum cryptography [32], quantum dense coding [33], and quantum teleportation [34]. Entangled two-qubit states that are based on the position-momentum entanglement of the down-converted photons are prepared by utilizing either the position or the momentum correlations of the down-converted photons [35–39]. When position correlations are used for the purpose, the prepared qubit states are referred to as spatial two-qubit states. Both Neves *et al.* [36,40] and O’sullivan *et al.* [35] have utilized the position correlations of down-converted photons to prepare entangled two-qubit states. The entanglement of spatial two-qubit states are quite often quantified by an entanglement measure called concurrence [41,42].

In the previous sections, we discussed how the spatial coherence properties of the two-photon field propagate and how they depend on the spatial coherence properties of the pump field. In this section, we study the connection between the degree of spatial two-photon-coherence and the entanglement of spatial two-qubit states as quantified by concurrence. We derive an explicit relationship showing how the entanglement of a spatial two-qubit state gets affected by the spatial coherence properties of the two-photon field, and in turn by the spatial coherence properties of the pump field. We restrict our analysis to the class of two-qubit states that can be represented by a density matrix having only two nonzero diagonal elements.

The scheme of Fig. 1(a) represents a spatial two-qubit state, with $\{|s1\rangle, |s2\rangle\}$ and $\{|i1\rangle, |i2\rangle\}$ forming the two-dimensional

orthonormal bases for the signal and idler photons, respectively, where $|s1\rangle$ represents the state of the signal photon passing through the hole located at transverse position ρ_{s1} , etc. The four-dimensional basis set for the two-qubit state can then be represented by $\{|s1\rangle|i1\rangle, |s1\rangle|i2\rangle, |s2\rangle|i1\rangle, |s2\rangle|i2\rangle\}$, where $|s1\rangle|i1\rangle$ represents the joint state of the signal and idler photons when the signal photon passes through the hole located at ρ_{s1} and the idler photon passes through the hole located at ρ_{i1} , etc.

We now make an explicit assumption that the probabilities of finding the signal and idler photons in states $|s1\rangle|i2\rangle$ and $|s2\rangle|i1\rangle$ are negligibly small. In an experiment, this can be ensured by keeping the separations between the two signal and the two idler holes to be much bigger than the two-photon correlation width $\sigma_s^{(2)}(z)$ so that the two-photon spectral densities for the pairs of transverse positions (ρ_{s1}, ρ_{i2}) and (ρ_{s2}, ρ_{i1}) are negligibly small. With the above assumption, the density matrix ρ_{qubit} of the two-qubit state thus prepared can be written in the basis $\{|s1\rangle|i1\rangle, |s1\rangle|i2\rangle, |s2\rangle|i1\rangle, |s2\rangle|i2\rangle\}$ as

$$\rho_{\text{qubit}} = \begin{pmatrix} a & 0 & 0 & c \\ 0 & 0 & 0 & 0 \\ 0 & 0 & 0 & 0 \\ d & 0 & 0 & b \end{pmatrix}, \quad (15)$$

where a and b are the probabilities that the signal and idler photons are detected in states $|s1\rangle|i1\rangle$ and $|s2\rangle|i2\rangle$, respectively, with $a + b = 1$. The off-diagonal term c is a measure of coherence between states $|s1\rangle|i1\rangle$ and $|s2\rangle|i2\rangle$, with $c = d^*$. From our studies in the last two sections, we find that the probability a of detecting the signal and idler photons in state $|s1\rangle|i1\rangle$ is proportional to the two-photon spectral density $S^{(2)}(\rho_1, z)$. Similarly, the probability b of detecting the signal and idler photons in state $|s2\rangle|i2\rangle$ is proportional to the two-photon spectral density $S^{(2)}(\rho_2, z)$. Thus, we write

$$a = \eta k_1^2 S^{(2)}(\rho_1, z) \quad \text{and} \quad (16)$$

$$b = \eta k_2^2 S^{(2)}(\rho_2, z), \quad (17)$$

where $\eta = 1/[k_1^2 S^{(2)}(\rho_1, z) + k_2^2 S^{(2)}(\rho_2, z)]$ is the constant of proportionality. Further, we find that the off-diagonal term c , which is a measure of coherence between the two-photon states $|s1\rangle|i1\rangle$ and $|s2\rangle|i2\rangle$, is proportional to the two-photon cross-spectral density $W^{(2)}(\rho_1, \rho_2, z) \equiv W^{(2)}(\rho_{s1}, \rho_{i1}, \rho_{s2}, \rho_{i2}, z)$ at the two pairs of transverse positions (ρ_{s1}, ρ_{i1}) and (ρ_{s2}, ρ_{i2}) , that is,

$$c = d^* = \eta k_1 k_2 W^{(2)}(\rho_1, \rho_2, z). \quad (18)$$

We now quantify the entanglement of the two-qubit state represented by the density matrix ρ_{qubit} . The entanglement of a general two-qubit state can be characterized in terms of Wootters' concurrence [41,42], which ranges from 0 to 1, with 1 corresponding to the maximally entangled two-qubit state and 0 to a nonentangled state. For a given two-qubit density matrix ρ , the concurrence $C(\rho)$ is given by $C(\rho) = \max\{0, \sqrt{\lambda_1} - \sqrt{\lambda_2} - \sqrt{\lambda_3} - \sqrt{\lambda_4}\}$. Here the λ_i 's are the non-negative eigenvalues, in descending order, of matrix $\zeta = \rho(\sigma_y \otimes \sigma_y)\rho^*(\sigma_y \otimes \sigma_y)$, with

$$\sigma_y = \begin{pmatrix} 0 & -i \\ i & 0 \end{pmatrix}$$

being the usual Pauli operator and ρ^* the complex conjugate of ρ . For the density matrix ρ_{qubit} , the matrix ζ becomes

$$\zeta = \begin{pmatrix} ab + cd & 0 & 0 & 2ac \\ 0 & 0 & 0 & 0 \\ 0 & 0 & 0 & 0 \\ 2bd & 0 & 0 & ab + cd \end{pmatrix}. \quad (19)$$

The eigenvalues of ζ in descending order are

$$\begin{aligned} \lambda_1 &= (\sqrt{ab} + |c|)^2, \\ \lambda_2 &= (\sqrt{ab} - |c|)^2, \\ \lambda_3 &= 0, \quad \text{and} \\ \lambda_4 &= 0, \end{aligned} \quad (20)$$

where we have substituted $c = d^*$. Thus, the concurrence $C(\rho_{\text{qubit}}) = \max\{0, \sqrt{\lambda_1} - \sqrt{\lambda_2} - \sqrt{\lambda_3} - \sqrt{\lambda_4}\}$ is given by

$$C(\rho_{\text{qubit}}) = 2|c| = \frac{2k_1 k_2 |W^{(2)}(\rho_1, \rho_2, z)|}{k_1^2 S^{(2)}(\rho_1, z) + k_2^2 S^{(2)}(\rho_2, z)}. \quad (21)$$

We thus find that for a spatial two-qubit state, concurrence is proportional to the magnitude of the two-photon cross-spectral density at the two pairs of transverse positions that define the two-qubit state. Using Eq. (12a), we rewrite the above expression as

$$C(\rho_{\text{qubit}}) = \frac{2k_1 k_2 \sqrt{S^{(2)}(\rho_1, z) S^{(2)}(\rho_2, z)}}{k_1^2 S^{(2)}(\rho_1, z) + k_2^2 S^{(2)}(\rho_2, z)} \mu^{(2)}(\Delta\rho, z). \quad (22)$$

Comparing Eq. (22) with Eq. (14), we at once see that the quantity on the right-hand side of Eq. (22) is the far-field visibility V of the two-photon interference fringes produced by the pair of double holes. This also implies that for a two-qubit state that has only two nonzero diagonal elements, entanglement can be characterized using a single experimentally measurable quantity [39]. In the special case in which $k_1^2 S^{(2)}(\rho_1, z) = k_2^2 S^{(2)}(\rho_2, z)$, or $a = b$, we get

$$C(\rho_{\text{qubit}}) = \mu^{(2)}(\Delta\rho, z); \quad (23)$$

that is, when the probabilities of detecting signal and idler photon in the two alternatives are equal, concurrence becomes equal to the degree of spatial two-photon-coherence. Since, as shown in the previous section, the degree of spatial two-photon coherence depends on the degree of spatial coherence of the pump field, it follows that the maximum achievable entanglement of a spatial two-qubit state is bounded by the degree of spatial coherence of the pump field.

We note that in our analysis we have not taken into account other factors that also affect phase-matching in PDC, such as the finite thickness of the nonlinear crystal and the finite frequency bandwidths of the fields, etc. As these factors do not introduce any decoherence in the down-conversion process, it is reasonable to assume that they do not affect the degree of coherence between the two alternatives. However, these factors do affect the two-photon spectral densities in the two alternatives. Therefore, in situations in which the two-photon spectral densities in the two alternatives are not equal, that is,

when $k_1^2 S^{(2)}(\boldsymbol{\rho}_1, z) \neq k_2^2 S^{(2)}(\boldsymbol{\rho}_2, z)$, the entanglement of the spatial two-qubit state is affected not only by the spatial coherence properties of the pump field but also by the aforementioned factors.

V. CONCLUSIONS AND DISCUSSION

In summary, we have studied the spatial coherence properties of the two-photon field produced by PDC when the pump field is, spatially, a partially coherent beam of the Gaussian Schell-model type. We have constructed two displacement parameters using the transverse position vectors of the signal and idler photons in the two interfering alternatives. In terms of these parameters, we have described two-alternative spatial two-photon interference and have shown that in PDC the spatial coherence properties of the pump field get entirely transferred to the spatial coherence properties of the down-converted two-photon field. We have then analyzed the effects due to the limited spatial coherence of the pump field on the entanglement of two-qubit states that are based on the spatial correlations of the two-photon field. We have shown that for such states the maximum achievable entanglement is bounded by the degree of spatial coherence of the pump field. One implication of the results of this article is that they allow one to determine how imperfect the spatial coherence properties of the pump laser can be while being sufficient to produce entangled light fields with specified degrees of entanglement.

Moreover, under certain circumstances, it might be desirable to generate entangled light fields with a less than complete degree of entanglement. For instance, it has been recently shown that spatially partially coherent beams are less affected by atmospheric turbulence than are spatially fully coherent beams [43–45]. In light of the results presented in this article, it then follows, at least intuitively, that the entangled two-photon field produced by using a partially coherent pump beam will be less susceptible to atmospheric turbulence than will the entangled two-photon field produced by using a fully coherent pump beam. This may have important implications in that the partial coherence of the pump field can be used as a parameter, along with the other phase-matching parameters, to prepare two-qubit states that are optimal for a given quantum-information protocol and a given strength of turbulence.

ACKNOWLEDGMENTS

We gratefully acknowledge financial support through a MURI grant from the US Army Research Office. We thank Emil Wolf for useful discussions and Shantanu Agarwal for explaining how to calculate concurrence.

APPENDIX

In this appendix, we calculate the two-photon cross-spectral density function $W^{(2)}(\boldsymbol{\rho}_{s1}, \boldsymbol{\rho}_{i1}, \boldsymbol{\rho}_{s2}, \boldsymbol{\rho}_{i2}, z)$ of Eq. (4b) for the case of nondegenerate PDC. Using Eqs. (5), (6), and (7), we

write Eq. (4b) as:

$$\begin{aligned} W^{(2)}(\boldsymbol{\rho}_{s1}, \boldsymbol{\rho}_{i1}, \boldsymbol{\rho}_{s2}, \boldsymbol{\rho}_{i2}, z) &= |A|^2 \iiint d\mathbf{q}_s d\mathbf{q}'_s d\mathbf{q}_i d\mathbf{q}'_i \langle V(\mathbf{q}_s + \mathbf{q}_i) V^*(\mathbf{q}'_s + \mathbf{q}'_i) \rangle_e \\ &\times e^{i(\mathbf{q}_s \cdot \boldsymbol{\rho}_{s1} - q_s^2 z / 2k_s + \mathbf{q}_i \cdot \boldsymbol{\rho}_{i1} - q_i^2 z / 2k_i)} \\ &\times e^{-i(\mathbf{q}'_s \cdot \boldsymbol{\rho}_{s2} - q_s'^2 z / 2k_s + \mathbf{q}'_i \cdot \boldsymbol{\rho}_{i2} - q_i'^2 z / 2k_i)}. \end{aligned} \quad (\text{A1})$$

We substitute for $\langle V(\mathbf{q}_s + \mathbf{q}_i) V^*(\mathbf{q}'_s + \mathbf{q}'_i) \rangle_e$ from Eq. (9) and calculate the far-field expression for $W^{(2)}(\boldsymbol{\rho}_{s1}, \boldsymbol{\rho}_{i1}, \boldsymbol{\rho}_{s2}, \boldsymbol{\rho}_{i2}, z)$, which after a very long but straightforward calculation can be shown to be

$$\begin{aligned} W^{(2)}(\boldsymbol{\rho}_{s1}, \boldsymbol{\rho}_{i1}, \boldsymbol{\rho}_{s2}, \boldsymbol{\rho}_{i2}, z) &= |A|^2 (2\pi A_p \sigma_s \delta k_s k_i / z^2)^2 \\ &\times \exp[(i/2z)(k_s \rho_{s1}^2 + k_i \rho_{i1}^2 - k_s \rho_{s2}^2 - k_i \rho_{i2}^2)] \\ &\times \exp\{-\alpha/z^2[(k_s \boldsymbol{\rho}_{s1} + k_i \boldsymbol{\rho}_{i1})^2 + (k_s \boldsymbol{\rho}_{s2} + k_i \boldsymbol{\rho}_{i2})^2] \\ &+ (2\beta/z^2)[(k_s \boldsymbol{\rho}_{s1} + k_i \boldsymbol{\rho}_{i1}) \cdot (k_s \boldsymbol{\rho}_{s2} + k_i \boldsymbol{\rho}_{i2})]\}. \end{aligned} \quad (\text{A2})$$

We substitute $k_0 = (k_s + k_i)$ and $k_d = (k_s - k_i)/2$, and writing $r_{s1} \approx z + \rho_{s1}^2/2z$, etc., we substitute $r'_1 = r_{s1} - r_{i1}$ and $r'_2 = r_{s2} - r_{i2}$. Finally, substituting for α and β from Eq. (9b), we write Eq. (A2) in terms of the two-photon transverse position vectors defined in Eq. (1):

$$\begin{aligned} W^{(2)}(\boldsymbol{\rho}_1, \boldsymbol{\rho}'_1, \boldsymbol{\rho}_2, \boldsymbol{\rho}'_2, z) &= e^{i[k_0(r_1 - r_2) + k_d(r'_1 - r'_2)]} \sqrt{S^{(2)}(\boldsymbol{\rho}_1, \boldsymbol{\rho}'_1, z) S^{(2)}(\boldsymbol{\rho}_2, \boldsymbol{\rho}'_2, z)} \\ &\times \mu^{(2)}(\Delta\boldsymbol{\rho}, \Delta\boldsymbol{\rho}', z), \end{aligned} \quad (\text{A3a})$$

where

$$\begin{aligned} S^{(2)}(\boldsymbol{\rho}_1, \boldsymbol{\rho}'_1, z) &= C_d \exp\{-(1/2)\{[\boldsymbol{\rho}_1 + (k_d/k_0)\boldsymbol{\rho}'_1]/\sigma_s^{(2)}(z)\}^2\} \end{aligned} \quad (\text{A3b})$$

is the two-photon spectral density in alternative 1, with $C_d = |A|^2 \{[A_p \pi \sigma_s \delta(k_0^2 - 4k_d^2)]/(2z^2)\}^2$, and where

$$\begin{aligned} \mu^{(2)}(\Delta\boldsymbol{\rho}, \Delta\boldsymbol{\rho}', z) &= \exp\{-(1/2)\{[\Delta\boldsymbol{\rho} + (k_d/k_0)\Delta\boldsymbol{\rho}']/\sigma_\mu^{(2)}(z)\}^2\} \end{aligned} \quad (\text{A3c})$$

is the degree of spatial two-photon-coherence. Now, using Eqs. (4) and (A3), we find the coincidence count rate $R_{si}(\mathbf{r}_s, \mathbf{r}_i)$ of Eq. (4a) to be

$$\begin{aligned} R_{si}(\mathbf{r}_s, \mathbf{r}_i) &= S^{(2)}(\boldsymbol{\rho}_1, \boldsymbol{\rho}'_1, z) + S^{(2)}(\boldsymbol{\rho}_2, \boldsymbol{\rho}'_2, z) \\ &+ 2\sqrt{S^{(2)}(\boldsymbol{\rho}_1, \boldsymbol{\rho}'_1, z) S^{(2)}(\boldsymbol{\rho}_2, \boldsymbol{\rho}'_2, z)} \\ &\times \mu^{(2)}(\Delta\boldsymbol{\rho}, \Delta\boldsymbol{\rho}', z) \cos(k_0 \Delta L + k_d \Delta L'), \end{aligned} \quad (\text{A4})$$

where we have substituted $\omega_0 = (\omega_s + \omega_i)$ and $\omega_d = (\omega_s - \omega_i)/2$, and have replaced $\omega_0 t_{s1}$ with $k_0 d_{s1}$ and $\omega_d t_{s1}$ with $k_d d_{s1}$, etc. We have also substituted $l_1 = r_1 + (d_{s1} + d_{i1})/2$, $l_2 = r_2 + (d_{s2} + d_{i2})/2$; $l'_1 = r'_1 + (d_{s1} - d_{i1})$, $l'_2 = r'_2 + (d_{s2} - d_{i2})$; and $\Delta L = l_1 - l_2$ and $\Delta L' = l'_1 - l'_2$. Here $l_{1(2)}$ is the two-photon path-asymmetry length in alternative 1 (2) [7]. We note that in the special case of degenerate down-conversion, $k_d = 0$, Eqs. (A3) and (A4) reduce to the corresponding Eqs. (12a) and (13), respectively, for the degenerate case.

- [1] C. K. Hong, Z. Y. Ou, and L. Mandel, *Phys. Rev. Lett.* **59**, 2044 (1987).
- [2] X. Y. Zou, L. J. Wang, and L. Mandel, *Phys. Rev. Lett.* **67**, 318 (1991).
- [3] T. J. Herzog, J. G. Rarity, H. Weinfurter, and A. Zeilinger, *Phys. Rev. Lett.* **72**, 629 (1994).
- [4] J. Brendel, E. Mohler, and W. Martienssen, *Phys. Rev. Lett.* **66**, 1142 (1991).
- [5] Z. Y. Ou, L. J. Wang, and L. Mandel, *Phys. Rev. A* **40**, 1428 (1989).
- [6] M. H. Rubin, D. N. Klyshko, Y. H. Shih, and A. V. Sergienko, *Phys. Rev. A* **50**, 5122 (1994).
- [7] A. K. Jha, M. N. O'Sullivan, K. W. C. Chan, and R. W. Boyd, *Phys. Rev. A* **77**, 021801(R) (2008).
- [8] W. P. Grice and I. A. Walmsley, *Phys. Rev. A* **56**, 1627 (1997).
- [9] T. E. Keller and M. H. Rubin, *Phys. Rev. A* **56**, 1534 (1997).
- [10] L. Mandel, *Phys. Rev. A* **28**, 929 (1983).
- [11] R. Ghosh, C. K. Hong, Z. Y. Ou, and L. Mandel, *Phys. Rev. A* **34**, 3962 (1986).
- [12] R. Ghosh and L. Mandel, *Phys. Rev. Lett.* **59**, 1903 (1987).
- [13] D. V. Strekalov, A. V. Sergienko, D. N. Klyshko, and Y. H. Shih, *Phys. Rev. Lett.* **74**, 3600 (1995).
- [14] M. D'Angelo, M. V. Chekhova, and Y. Shih, *Phys. Rev. Lett.* **87**, 013602 (2001).
- [15] C. K. Hong and T. G. Noh, *J. Opt. Soc. Am. B* **15**, 1192 (1998).
- [16] G. Brida, E. Cagliero, G. Falzetta, M. Genovese, M. Gramegna, and E. Predazzi, *Phys. Rev. A* **68**, 033803 (2003).
- [17] E. J. S. Fonseca, J. C. Machado da Silva, C. H. Monken, and S. Pádua, *Phys. Rev. A* **61**, 023801 (2000).
- [18] C. K. Hong and L. Mandel, *Phys. Rev. A* **31**, 2409 (1985).
- [19] M. H. Rubin, *Phys. Rev. A* **54**, 5349 (1996).
- [20] C. H. Monken, P. H. Souto Ribeiro, and S. Pádua, *Phys. Rev. A* **57**, 3123 (1998).
- [21] A. Joobeur, B. E. A. Saleh, T. S. Larchuk, and M. C. Teich, *Phys. Rev. A* **53**, 4360 (1996).
- [22] P. H. Souto Ribeiro, *Phys. Rev. A* **56**, 4111 (1997).
- [23] E. J. S. Fonseca, C. H. Monken, S. Pádua, and G. A. Barbosa, *Phys. Rev. A* **59**, 1608 (1999).
- [24] B. E. A. Saleh, M. C. Teich, and A. V. Sergienko, *Phys. Rev. Lett.* **94**, 223601 (2005).
- [25] W. H. Carter and E. Wolf, *Opt. Acta* **28**, 227 (1981).
- [26] L. Mandel and E. Wolf, *Optical Coherence and Quantum Optics* (Cambridge University Press, New York, 1995).
- [27] M. Born and E. Wolf, *Principles of Optics* (Cambridge University Press, Cambridge, 1999), 7th expanded edition.
- [28] R. J. Glauber, *Phys. Rev.* **130**, 2529 (1963).
- [29] E. W. Marchand and E. Wolf, *J. Opt. Soc. Am.* **62**, 379 (1972).
- [30] C. Kim, R.-D. Li, and P. Kumar, *Opt. Lett.* **19**, 132 (1994).
- [31] A. K. Jha, M. Malik, and R. W. Boyd, *Phys. Rev. Lett.* **101**, 180405 (2008).
- [32] A. K. Ekert, *Phys. Rev. Lett.* **67**, 661 (1991).
- [33] C. H. Bennett and S. J. Wiesner, *Phys. Rev. Lett.* **69**, 2881 (1992).
- [34] C. H. Bennett, G. Brassard, C. Crépeau, R. Jozsa, A. Peres, and W. K. Wootters, *Phys. Rev. Lett.* **70**, 1895 (1993).
- [35] M. N. O'Sullivan Hale, I. A. Khan, R. W. Boyd, and J. C. Howell, *Phys. Rev. Lett.* **94**, 220501 (2005).
- [36] L. Neves, G. Lima, E. J. S. Fonseca, L. Davidovich, and S. Pádua, *Phys. Rev. A* **76**, 032314 (2007).
- [37] S. P. Walborn and C. H. Monken, *Phys. Rev. A* **76**, 062305 (2007).
- [38] G. Taguchi, T. Dougakiuchi, N. Yoshimoto, K. Kasai, M. Iinuma, H. F. Hofmann, and Y. Kadoya, *Phys. Rev. A* **78**, 012307 (2008).
- [39] A. K. Jha, J. Leach, B. Jack, S. Franke-Arnold, S. M. Barnett, R. W. Boyd, and M. J. Padgett, *Phys. Rev. Lett.* **104**, 010501 (2010).
- [40] L. Neves, G. Lima, J. G. Aguirre Gómez, C. H. Monken, C. Saavedra, and S. Pádua, *Phys. Rev. Lett.* **94**, 100501 (2005).
- [41] S. Hill and W. K. Wootters, *Phys. Rev. Lett.* **78**, 5022 (1997).
- [42] W. K. Wootters, *Phys. Rev. Lett.* **80**, 2245 (1998).
- [43] G. Gbur and E. Wolf, *J. Opt. Soc. Am. A* **19**, 1592 (2002).
- [44] T. Shirai, A. Dogariu, and E. Wolf, *J. Opt. Soc. Am. A* **20**, 1094 (2003).
- [45] M. Salem, T. Shirai, A. Dogariu, and E. Wolf, *Opt. Commun.* **216**, 261 (2003).